

# Fragmentation function and hadronic production of the heavy supersymmetric hadrons

Chao-Hsi Chang<sup>1,2,4,a</sup>, Jiao-Kai Chen<sup>2,3,b</sup>, Zhen-Yun Fang<sup>4,c</sup>, Bing-Quan Hu<sup>4</sup>, Xing-Gang Wu<sup>2,4,d</sup>

<sup>1</sup> CCAST (World Laboratory), P.O. Box 8730, Beijing 100080, P.R. China

<sup>2</sup> Institute of Theoretical Physics, Chinese Academy of Sciences, P.O. Box 2735, Beijing 100080, P.R. China

<sup>3</sup> Department of Mathematics and Physics, Henan University of Science and Technology, Luoyang, P.R. China, 471003

<sup>4</sup> Department of Physics, Chongqing University, Chongqing, 400044, P.R. China

Received: 17 February 2006 / Revised version: 17 November 2006 /

Published online: 7 March 2007 – © Springer-Verlag / Società Italiana di Fisica 2007

**Abstract.** The light top-squark  $\tilde{t}_1$  may be the lightest squark, and its lifetime may be ‘long enough’ in a kind of SUSY models that have not been ruled out yet experimentally, so colorless ‘supersymmetric hadrons (superhadrons)’ ( $\tilde{t}_1 \bar{q}$ ) ( $q$  is a quark excluding the  $t$ -quark) may be formed as long as the light top-squark  $\tilde{t}_1$  can be produced. The fragmentation function of  $\tilde{t}_1$  into heavy ‘supersymmetric hadrons (superhadrons)’ ( $\tilde{t}_1 \bar{Q}$ ) ( $\bar{Q} = \bar{c}$  or  $\bar{b}$ ) and hadronic production of the superhadrons are investigated quantitatively. The fragmentation function is calculated precisely. Due to the difference in spin of the SUSY component, the asymptotic behavior of the fragmentation function is different from those of the existing ones. The fragmentation function is also applied to compute the production of heavy superhadrons at the hadronic colliders Tevatron and LHC in the so-called fragmentation approach. The resultant cross-section for the heavy superhadrons is too small to observe at Tevatron, but large enough at LHC, when all the relevant parameters in the SUSY models are taken within the favored region for the heavy superhadrons. The production of ‘light superhadrons’ ( $\tilde{t}_1 \bar{q}$ ) ( $q = u, d, s$ ) is also roughly estimated with the same SUSY parameters. It is pointed out that the production cross-sections of the light superhadrons ( $\tilde{t}_1 \bar{q}$ ) may be much greater than those of the heavy superhadrons, so that even at Tevatron the light superhadrons may be produced in great quantities.

**PACS.** 12.38.Bx; 13.87.Fh; 12.60.Jv; 14.80.Ly

## 1 Introduction

Supersymmetry (SUSY) is one of the most appealing extensions of the standard model (SM) [1–5]. Without knowing the actual SUSY breaking mechanism, even in the minimum supersymmetry extension of the standard model (MSSM), there are too many parameters in the SUSY sector that need to be fixed via experimental measurements. If the MSSM is rooted in the ‘minimum supergravity model’ (mSUGRA), the numbers of independent parameters can be well deduced, but there are still many un-fixed parameters [5–7]. Therefore, the spectrum of the SUSY sector in SUSY models still is an open problem.<sup>1</sup>

For some kinds of SUSY models and by choosing un-fixed parameters from the region that has not been ruled out yet, it is not difficult to realize a general feature of the two mass eigenstates  $\tilde{t}_1$  and  $\tilde{t}_2$  for the SUSY partners of top-quark (top-squark  $\tilde{t}_L$  and  $\tilde{t}_R$ ) such that the comparatively lighter one  $\tilde{t}_1$  is the lightest squark, and the lifetime of  $\tilde{t}_1$  is so ‘long’ that its width is less than  $\Lambda_{\text{QCD}}$  [8–15]. In this case,  $\tilde{t}_1$  may form various colorless hadrons, i.e. the superhadrons by the QCD interaction, which consist of  $\tilde{t}_1$  and  $\bar{q}$  (here  $q = u, d, c, s, b$ ). On the other hand, a direct experimental search for the SUSY partners may only set a lower bound on the mass of  $\tilde{t}_1$ :  $m_{\tilde{t}_1} \geq 100 \text{ GeV}$  [17, 18]<sup>2</sup> (even lower than 75 GeV [15]). Therefore, in the paper, we would like to focus our attention on the consequences for the possible features of  $\tilde{t}_1$ . Namely, we shall assume that  $\tilde{t}_1$ , the SUSY partner of the top-quark, is not very heavy, e.g.  $m_{\tilde{t}_1} \simeq 120 \sim 150 \text{ GeV}$ , and that it has a ‘quite long’ lifetime,  $\Gamma_{\tilde{t}_1} \leq \Lambda_{\text{QCD}}$ , so that  $\tilde{t}_1$  (after having been produced and before decaying) has a chance to form colorless

<sup>a</sup> e-mail: zhangzx@itp.ac.cn

<sup>b</sup> e-mail: jkch@mail.haust.edu.cn

<sup>c</sup> e-mail: zyfang@cqu.edu.cn

<sup>d</sup> e-mail: wuxg@itp.ac.cn

<sup>1</sup> In fact, all of the available indications on the masses of the SUSY partners are abstracted from experimental measurements and/or astro-observations under assumptions (not direct measurements), so one should consider them only as references.

<sup>2</sup> For a summary see [16].

superhadrons ( $\tilde{t}_1\bar{q}$ ).<sup>3</sup> Moreover, we think that the squark (antisquark) in the superhadrons is a scalar, which is different from a quark in the ‘common’ hadrons; hence with such a scalar component the study of the superhadrons is also very interesting from the point of view of the bound state.

There was remarkable progress in the nineties of the previous century in perturbative QCD (pQCD) in double heavy meson studies, i.e., it was realized that the fragmentation function and the production of a double heavy meson such as  $B_c$  and  $\eta_c$  or  $J/\psi$  can be reliably computed in terms of pQCD and the wavefunction derived from the potential model [22–28],<sup>4</sup> and further progress in formulating the problem under the framework of the effective theory: non-relativistic QCD (NRQCD) [29, 30] was made a couple years later. We should note here that before [22–28] there were papers [31, 32]. The inclusive production of a meson [31, 32] and the fragmentation functions of a parton into a meson [32] were calculated. But the authors of [32] precisely claimed that their calculations might be extended to the cases for the heavy–light mesons, such as  $D, B$  etc. In fact, the claim is incorrect and misleading in the key point on the theoretical calculability of the production and the fragmentation functions.<sup>5</sup> Since heavy–light mesons contain a light quark, and the light quark creation involved in the fragmentation function is non-perturbative, it cannot be further factorized out as a hard factor as that in the case of the double heavy mesons. This is just the reason why, similar to the case for double heavy mesons, we expect that only the ‘heavy superhadrons’ ( $\tilde{t}_1\bar{Q}$ ) (but not the ‘light superhadrons’ ( $\tilde{t}_1\bar{q}$ )), where  $Q$  ( $q$ ) denotes a heavy quark,  $c$  or  $b$ , (a light quark,  $u$  or  $d$  or  $s$ ), and their inclusive production and fragmentation functions may be calculated reliably. The fragmentation functions for the ‘heavy superhadrons’ ( $\tilde{t}_1\bar{Q}$ ) can simply be attributed to the wavefunction of the potential model and a pQCD calculable factor as in the case of the double heavy mesons.

For the ‘light superhadrons’ ( $\tilde{t}_1\bar{q}$ ), where  $q$  indicates a light quark,  $u, d$  or  $s$ , due to the non-perturbative nature for producing the light quark  $q$  involved, the ‘story’ about the calculation of the fragmentation functions is

very different, i.e., the fragmentation functions cannot be attributed to a wavefunction and a hard factor of pQCD. Due to the non-perturbative QCD effects in the fragmentation functions of the ‘light–heavy mesons’ such as  $B, D$  etc., so far practically the only way to obtain the fragmentation functions of the ‘light–heavy meson’ is to first have a formulation in terms of theoretical considerations and a parametrization; then the parameters in the formulation are fixed via experimental measurement(s). With the fragmentation functions the production cross-section of a ‘light–heavy meson’, as experience tells us, generally is greater than that of the respective double heavy meson (the quark  $q$  in a ‘light–heavy meson’ is replaced by a charm-quark  $c$ ) by a factor of  $10^{3\sim 4}$ . Since there are no experimental observations of superhadrons, we cannot follow the same way for the ‘light superhadrons’ as for ‘light–heavy mesons’ at all. Alternatively, as an order of magnitude estimate, we expect that the fragmentation function and the production of the light superhadrons ( $\tilde{t}_1\bar{q}$ ) are also greater than that of the respective heavy superhadrons ( $\tilde{t}_1\bar{Q}$ ) by a factor of  $10^{3\sim 4}$ , no matter how heavy  $\tilde{t}_1$  is; that is very similar to the case of a double heavy meson versus a heavy–light meson. Thus, based on the quantitative computation of the fragmentation function and the production of the heavy superhadrons, we simply extend the results of the production to the light superhadrons at the end of the paper by referring to the cases of the ‘double heavy mesons’ versus the ‘light–heavy mesons’ as agrees with our experience. For convenience, we will denote ( $\tilde{t}_1\bar{Q}$ ) as  $\tilde{H}$  throughout the paper. Since the spectrum and the wavefunction respectively of a double heavy quark binding system, i.e. a system of a heavy quark and a heavy antiquark, ( $Q'\bar{Q}$ ), can be quite well obtained theoretically in terms of the non-relativistic potential model inspired on QCD, the ‘heavy superhadrons’  $\tilde{H}$ , as the double heavy systems ( $Q'\bar{Q}$ ), may also be depicted by the non-relativistic potential model as long as the difference in spin is carefully taken into account [20, 21]. Therefore, there is no problem to obtain the wavefunctions of the ‘heavy superhadrons’  $\tilde{H}$  that appear in the fragmentation functions.

In the literature, there are two approaches for estimating direct production of a double heavy meson in the NRQCD framework: the ‘fragmentation approach’ versus the complete ‘lowest-order-calculation’ approach. It is known that, of the two approaches, the former is much simpler than the latter in computation, but the former is ‘good’ only in the region where the transverse momentum of the produced double heavy meson is large ( $p_T \gtrsim 15$  GeV) [33–35]. The situation for the production of the heavy superhadrons is similar to the cases of the double heavy mesons, so, of the two approaches, we adopt the fragmentation approach when estimating the production of the superhadrons for rough estimation.

This paper is organized as follows. In Sect. 2, we show how to derive the fragmentation function of the lightest top-squark  $\tilde{t}_1$  into the ‘heavy superhadrons’  $\tilde{H}$ , and we try to properly present the results obtained, i.e. its general features. In Sect. 3, we compute the cross-sections for hadronic production of the superhadrons at the Tevatron

<sup>3</sup> This kind of superhadrons are bound states of a quark (antiquark) and an antisquark (squark), or two gluinos, or two quarks (antiquarks) and a squark (antisquark), etc. All of them are colorless and are bound via the strong interaction (QCD) [19–21].

<sup>4</sup> To be exact, here we mean the color-singlet mechanism only; i.e. only the color-singlet component of the double heavy meson concerned, which is the biggest in a Fock space expansion, is taken into account in calculating the fragmentation function and production as well. Since the color-octet matrix element appearing in the formulation for the color-octet mechanism production (fragmentation function) could not be calculated theoretically so far, the color-octet mechanism is not the opportune case.

<sup>5</sup> To present the calculations of the fragmentation functions, here we would like also to recall that there are some substantial contributions from the phase-space integration that might be missed if not enough care is taken. In fact, as pointed out in [23], they were missed in [32] indeed.

and LHC colliders in terms of the so-called fragmentation approach. Section 4 is devoted to a discussion and conclusions.

## 2 Fragmentation function of the light top-squark $\tilde{t}_1$ to the heavy superhadrons $\tilde{H}$

In this paper we adopt the fragmentation approach to estimate the  $\tilde{H}$  production, and in the present section we compute the fragmentation function first; it is one of the key factors of the fragmentation approach.

According to pQCD, with leading logarithmic (LL) terms being summed over, the fragmentation function of a ‘parton’  $i$  into a heavy superhadron  $\tilde{H}$  is depicted by the DGLAP equation as follows [36–38]:

$$\frac{dD_{i \rightarrow \tilde{H}}(z, Q^2)}{d\tau} = \sum_j \frac{\alpha_s(Q^2)}{2\pi} \int_z^1 \frac{dy}{y} P_{i \rightarrow j}(z/y) D_{j \rightarrow \tilde{H}}(y, Q^2), \quad (1)$$

where  $\tau = \log(Q^2/\Lambda_{\text{QCD}}^2)$ , and  $P_{i \rightarrow j}(x)$  is the splitting function. For example, the splitting function for the supersymmetric top-squark [39, 40] reads

$$P_{\tilde{t}_1 \rightarrow \tilde{t}_1 g}(x) = \frac{4}{3} \left[ \frac{1+x^2}{(1-x)_+} - (1-x) + \delta(1-x) \right].$$

Since (1) is an integro-differential equation, to have a definite solution, a ‘boundary (initial) condition’ for the equation, i.e.  $D_{j \rightarrow \tilde{H}}(z, Q_0)$ , the fragmentation function at the energy scale  $Q_0 \simeq m_{\tilde{t}_1}$ , is needed. Now the task is to obtain the boundary condition. Fortunately, the boundary condition for the heavy superhadron  $\tilde{H}$  can be derived in terms of pQCD and the relevant wavefunction precisely like for double heavy mesons [22–28]. Hereafter, to simplify our notation, we shall always use  $D_{j \rightarrow \tilde{H}}(z)$  instead of  $D_{j \rightarrow \tilde{H}}(z, Q_0)$ .

Since the fragmentation functions are universal by definition, i.e. they are independent of the concrete process, for the ‘boundary (initial) condition’ of the fragmentation function of the light top-squark  $\tilde{t}_1$ , we would like to choose a relevant simple process to calculate the ‘boundary condition’  $D_{\tilde{t}_1 \rightarrow \tilde{H}}(z)$ . In order to simplify the derivation as much as possible, we furthermore assume a fictitious “ $Z$ ” that, except for the mass, has the same properties as that of the physical  $Z$  boson. The fictitious “ $Z$ ” has such a great mass that it may decay to a  $\tilde{t}_1$  and  $\bar{\tilde{t}}_1$  pair.

According to the pQCD factorization theorem, the differential width for the fictitious “ $Z$ ” into  $\tilde{H}$  may be factorized as

$$d\Gamma(\text{“}Z\text{”} \rightarrow \tilde{H} + X) = \int_0^1 dz d\hat{\Gamma}(\text{“}Z\text{”} \rightarrow \tilde{t}_1 + \bar{\tilde{t}}_1, \mu_f) D_{\tilde{t}_1 \rightarrow \tilde{H}}(z, \mu_f), \quad (2)$$

where  $z = \frac{2E}{\sqrt{s_{\text{eff}}}}$ , and  $\mu_f$  is the energy scale for factorization. By definition,  $D_{\tilde{t}_1 \rightarrow \tilde{H}}(z, \mu_f)$  is the fragmentation function, which represents the probability of  $\tilde{t}_1$  to fragment into a superhadron with energy fraction  $z$ .

To calculate  $D_{\tilde{t}_1 \rightarrow \tilde{H}}(z)$ , let us calculate the process “ $Z$ ”  $\rightarrow \tilde{H} + X$  precisely. Of the lowest-order pQCD calculation, the Feynman diagrams for the inclusive decay of the fictitious particle “ $Z$ ” into a  $(\frac{1}{2})^-$  superhadron  $\tilde{H}$  (with mass  $M$ ), “ $Z$ ”  $\rightarrow \tilde{H} + X$ , are described by the three diagrams (A), (B) and (C) as shown in Fig. 1. The intermediate gluon in each of the Feynman diagrams should ensure the production of a heavy quark–antiquark pair, so its momentum squared should be bigger than  $(p_2 + q_2)^2 \geq 4m_Q^2 \gg \Lambda_{\text{QCD}}^2$ , thus the pQCD calculation and the factorization theorem are reliable. The corresponding amplitudes are

$$M = \frac{4g_s^2}{3\sqrt{3}} \frac{gc_{11}}{\cos\theta_W} \int d^4q \text{Tr} \left\{ \chi^{(1/2)-}(p, q) (h_A^\mu + h_B^\mu + h_C^\mu) \times \frac{G_{\mu\nu}}{(p_2 + q_2)^2} \bar{u}(q_2) \gamma^\nu \right\} \\ \simeq \frac{4g_s^2}{3\sqrt{3}} \frac{gc_{11}}{\cos\theta_W} g_B (h_A^\mu + h_B^\mu + h_C^\mu) \frac{G_{\mu\nu}}{(p_2 + q_2)^2} L^\nu, \quad (3)$$

with

$$h_A^\mu = \frac{(p_1 + k - q_1)^\mu}{(k - q_1)^2 - m_{\tilde{t}_1}^2} (k - 2q_1) \cdot \epsilon, \\ h_B^\mu = -2\epsilon^\mu, \\ h_C^\mu = \frac{(p_1 - k - q_1)^\mu}{(k - p_1)^2 - m_{\tilde{t}_1}^2} (2p_1 - k) \cdot \epsilon$$

and

$$L^\nu = \bar{u}(q_2) \gamma^\nu v(p), \\ G_{\mu\nu} = g_{\mu\nu} - \frac{q_{1\mu}(q_2 + p_2)_\nu + q_{1\nu}(q_2 + p_2)_\mu}{q_1(q_2 + p_2)}, \\ g_B = \frac{\phi(0)}{2\sqrt{m_{\tilde{t}_1}}},$$

where  $k$ ,  $p_1$ ,  $p_2$ ,  $q_1$  and  $q_2$  are the four-momenta of “ $Z$ ”, top-squark  $\tilde{t}_1$ , antiquark  $\bar{Q}$  ( $\bar{b}$  or  $\bar{c}$ ), top-antisquark  $\bar{\tilde{t}}_1$  and

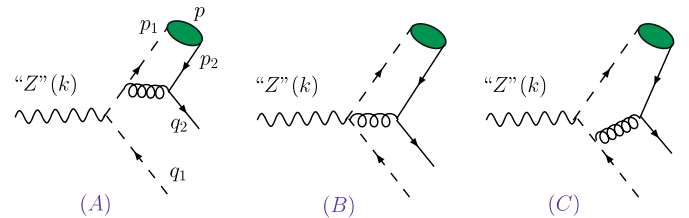


**Fig. 1.** The Feynman diagrams for the fictitious particle “ $Z(k)$ ” decaying into a superhadron  $\tilde{H}(p)$ ,  $\tilde{t}_1(q_1)$  and  $b(q_2)$  (a bottom quark) or  $c_1(q_2)$  (a charm quark). (A), (B), (C) are the Feynman diagrams with the hard virtual gluon attached to the light top-squark  $\tilde{t}_1$  and its anti-particle  $\bar{\tilde{t}}_1$  in different ways

quark  $Q$  ( $b$  or  $c$ ), respectively.  $p$  is the four-momentum of  $\tilde{H}$ , and  $q$  is the relative momentum of the two constituents inside  $\tilde{H}$ , so we have  $p = p_1 + p_2$ ,  $q = \alpha_2 p_1 - \alpha_1 p_2$  with  $\alpha_1 = \frac{m_1}{m_1 + m_2}$ ,  $\alpha_2 = \frac{m_2}{m_1 + m_2}$ , where  $m_1$  and  $m_2$  are the masses of  $\tilde{t}_1$ ,  $\bar{Q}$ , respectively.  $\phi(0)$  is the wavefunction at the origin for the superhadron  $\tilde{H}$ . On neglecting the  $q$ -dependence of the integrand of (3), which can be considered as the lowest term in the expansion of  $q$  for the integrand, all the non-perturbative effects can be attributed to the wavefunction at the origin after doing the integration over  $q$ .  $\epsilon$  is the polarization vector for the fictitious particle “ $Z$ ”.  $c_{11} = I_{3L} \cos^2 \theta_{\tilde{q}} - e_q \sin^2 \theta_W$  [41].<sup>6</sup> For convenience, the variables  $S_{\text{eff}} = k^2$ ,  $x = \frac{2p \cdot k}{S_{\text{eff}}}$ ,  $y = \frac{2q_1 \cdot k}{S_{\text{eff}}}$ ,  $z = \frac{2q_2 \cdot k}{S_{\text{eff}}}$ ,  $M = m_{\tilde{t}_1} + m_Q$  and  $d = \frac{M}{\sqrt{S_{\text{eff}}}}$  are introduced. Keeping the leading term for  $d^2$ , the maximum and minimum values of  $y$  are  $y_{\text{max}} = 1 - \frac{d^2(1-\alpha_1 x)^2}{x(1-x)}$ ,  $y_{\text{min}} = 1 - x + \frac{d^2(1-x+\alpha_1 x)^2}{x(1-x)}$ . In the calculation, the axial gauge  $n_\mu = q_{1\mu}$  is adopted. Under the axial gauge, it can be found that only the two amplitudes  $M_A$  and  $M_B$ , which correspond to the first two Feynman diagrams in Fig. 1, have contributions to the fragmentation function.

According to the factorization (2), the fragmentation function versus  $z$  at the energy scale  $Q_0$  can be derived by dividing the differential decay width by  $\Gamma_0$ :

$$D_{\tilde{t}_1 \rightarrow \tilde{H}}(z) = \frac{1}{\Gamma_0} \frac{d\Gamma}{dz}, \quad (4)$$

where  $\Gamma_0$  is the decay width for the fictitious particle “ $Z$ ” into the top-squark  $\tilde{t}_1$  and the top-antisquark  $\bar{\tilde{t}_1}$ . Thus the result for the fragmentation function may be presented as follows:

$$D_{\tilde{t}_1 \rightarrow \tilde{H}}(z) = F_{\tilde{t}_1} \cdot f_{\tilde{t}_1}(z), \quad (5)$$

where

$$F_{\tilde{t}_1} = \frac{16\alpha_s(4m_Q^2)|\phi(0)|^2}{27\pi m_Q^2 m_{\tilde{t}_1}},$$

$$f_{\tilde{t}_1}(z) = \frac{1}{6} \frac{(1-z)^2 z^2}{(1-\alpha_1 z)^6} \left[ 2\alpha_1^2(z-4)z + \alpha_1^3(3\alpha_1 z - 2z + 2)z + 3\alpha_1^2 - 6\alpha_1 + 6 \right]. \quad (6)$$

At present, there are no experimental data for the superhadron at all, so we adopt a potential model with the Cornell potential  $(-\frac{\kappa}{r} + \frac{a}{a^2})$  to estimate the wavefunction at the origin,  $\phi(0)$ . For definiteness, we assume that the potential of the heavy scalar–antiquark binding system is the same as that of double heavy–quark–antiquark systems. The relevant parameters are taken as  $\kappa = 0.52$ ,  $a = 2.34 \text{ GeV}^{-1}$  [42],  $m_{\tilde{t}_1} = 120$  or  $150 \text{ GeV}$ ,  $m_b = 5.18 \text{ GeV}$  and  $m_c = 1.84 \text{ GeV}$ . The corresponding wavefunctions at

**Table 1.** The wavefunction at the origin,  $\phi(0)$ , for  $(\tilde{t}_1 \bar{b})$  or  $(\tilde{t}_1 \bar{c})$ . The parameters are  $m_b = 5.18 \text{ GeV}$  and  $m_c = 1.84 \text{ GeV}$

$m_{\tilde{t}_1}$	120 GeV	150 GeV
$\phi(0)_{(\tilde{t}_1 \bar{b})} [(\text{GeV})^{3/2}]$	2.502	2.530
$\phi(0)_{(\tilde{t}_1 \bar{c})} [(\text{GeV})^{3/2}]$	0.693	0.695

the origin  $\phi(0)$  for the system  $(\tilde{t}_1 \bar{b})$  and  $(\tilde{t}_1 \bar{c})$  are listed in Table 1.

The fragmentation function obtained,  $D_{\tilde{t}_1 \rightarrow \tilde{H}}(z)$ , see (5), is just a boundary condition for the DGLAP evolution equation (1). Solving the DGLAP equation, one may obtain the fragmentation function with the energy-scale evolution to  $Q^2$ . The relevant Feynman diagrams for the boundary condition  $D_{j \rightarrow \tilde{H}}(z)$  with  $(j = q, \bar{q}, g)$  are of higher order in  $\alpha_s$  than the Feynman diagrams for  $D_{\tilde{t}_1 \rightarrow \tilde{H}}(z)$ , see Fig. 1;<sup>7</sup> therefore, only the case with  $i, j = \tilde{t}_1$  shall be taken into account in solving (1), so as to meet the LL approximation criterion.

We solve (1) with the method developed by Field [43]. When  $Q^2 \gg m_{\tilde{t}_1}^2$ , according to [43] we have the following solution:

$$D_{\tilde{t}_1 \rightarrow \tilde{H}}(z, Q^2) = \tilde{D}_{\tilde{t}_1 \rightarrow \tilde{H}}\left(\frac{8}{3}, z, Q^2\right) + \kappa \int_z^1 \frac{dy}{y} \tilde{D}_{\tilde{t}_1 \rightarrow \tilde{H}}\left(\frac{8}{3}, z/y, Q^2\right) P_{\Delta}(y) + \kappa \int_z^1 \frac{dy}{y} \tilde{D}_{g \rightarrow \tilde{H}}(z/y, Q^2) P_{\tilde{t}_1 \rightarrow g}(y) + O(\kappa^2),$$

$$D_{g \rightarrow \tilde{H}}(z, Q^2) = \tilde{D}_{g \rightarrow \tilde{H}}(6, z, Q^2) + \kappa \int_z^1 \frac{dy}{y} \tilde{D}_{g \rightarrow \tilde{H}}(6, z/y, Q^2) P_{\Delta g}(y) + \kappa \int_z^1 \frac{dy}{y} \tilde{D}_{\tilde{t}_1 \rightarrow \tilde{H}}(z/y, Q^2) P_{g \rightarrow \tilde{t}_1}(y) + O(\kappa^2), \quad (7)$$

with

$$P_{\Delta}(x) = \frac{4}{3} \left[ \frac{1+x^2}{1-x} + \frac{2}{\log(x)} + \left( \frac{3}{2} - 2\gamma_E \right) \delta(1-x) - (1-x) \right],$$

<sup>6</sup>  $c_{11}$  is a factor in the effective “ $Z''-\tilde{t}_1-\bar{\tilde{t}_1}$ ” coupling, which will not appear in the final result of the fragmentation function because of cancellation between the numerator and denominator in (4).

<sup>7</sup> For  $D_{g \rightarrow \tilde{H}}(z)$ , the relevant part of the Feynman diagrams must have one more strong coupling vertex ( $g \rightarrow \tilde{t}_1 \bar{\tilde{t}_1}$ ) in  $\alpha_s$  than the relevant part  $\tilde{t}_1 \rightarrow \tilde{H}$  in Fig. 1, and for  $D_{q(\bar{q}) \rightarrow \tilde{H}}(z)$  the relevant Feynman diagrams must have two more strong coupling vertices  $q \rightarrow qg$  and  $g \rightarrow \tilde{t}_1 \bar{\tilde{t}_1}$  in  $\alpha_s$  than those for  $\tilde{t}_1 \rightarrow \tilde{H}$ .

$$P_{\Delta g}(x) = 6 \left[ \frac{x}{1-x} + \frac{1}{\log(x)} + \frac{1-x}{x} + x(1-x) + \left( \frac{11}{12} - \frac{1}{18}n_f - \gamma_E \right) \delta(1-x) \right] \quad (8)$$

and

$$\begin{aligned} \tilde{D}_{\tilde{t}_1 \rightarrow \tilde{H}}(a, z, Q^2) &\equiv \int_z^1 \frac{dy}{y} D_{\tilde{t}_1 \rightarrow \tilde{H}}(z/y, Q_0^2) \frac{(-\log(y))^{(a\kappa-1)}}{\Gamma(a\kappa)}, \\ \tilde{D}_{g \rightarrow \tilde{H}}(b, z, Q^2) &\equiv \int_z^1 \frac{dy}{y} D_{g \rightarrow \tilde{H}}(z/y, Q_0^2) \frac{(-\log(y))^{(b\kappa-1)}}{\Gamma(b\kappa)}, \\ \tilde{\tilde{D}}_{\tilde{t}_1 \rightarrow \tilde{H}}(z, Q^2) &\equiv \frac{1}{6 - \frac{8}{3}} \int_{\frac{8}{3}}^6 da D_{\tilde{t}_1 \rightarrow \tilde{H}}(a, z, Q^2), \\ \tilde{\tilde{D}}_{g \rightarrow \tilde{H}}(z, Q^2) &\equiv \frac{1}{6 - \frac{8}{3}} \int_{\frac{8}{3}}^6 db D_{g \rightarrow \tilde{H}}(b, z/y, Q^2), \end{aligned}$$

where  $\kappa = \frac{6}{33-2n_f} \log(\alpha_s(Q_0^2)/\alpha_s(Q^2))$ , where  $\gamma_E$  is the Euler constant. Furthermore, at LL level we have the boundary condition  $D_{g \rightarrow \tilde{H}}(z/y, Q_0^2) = 0$ ; thus the solution (7) becomes

$$\begin{aligned} D_{\tilde{t}_1 \rightarrow \tilde{H}}(z, Q^2) &= \tilde{D}_{\tilde{t}_1 \rightarrow \tilde{H}}\left(\frac{8}{3}, z, Q^2\right) \\ &\quad + \kappa \int_z^1 \frac{dy}{y} \tilde{D}_{\tilde{t}_1 \rightarrow \tilde{H}}\left(\frac{8}{3}, z/y, Q^2\right) P_{\Delta}(y) \\ &\quad + O(\kappa^2), \\ D_{g \rightarrow \tilde{H}}(z, Q^2) &= \kappa \int_z^1 \frac{dy}{y} \tilde{\tilde{D}}_{\tilde{t}_1 \rightarrow \tilde{H}}(z/y, Q^2) P_{g \rightarrow \tilde{t}_1}(y) \\ &\quad + O(\kappa^2). \end{aligned} \quad (9)$$

Numerically, it can be found that the first term for  $D_{\tilde{t}_1 \rightarrow \tilde{H}}(z, Q^2)$  is much greater than the other terms on the right hand side of the first equation of (9), and then it is quite accurate to consider the first term only. Moreover, due to the fact that the splitting function  $P_{g \rightarrow \tilde{t}_1 \tilde{t}_1^*}$  must be greatly suppressed being  $\mathcal{O}(m_Q^2/m_{\tilde{t}_1}^2)$  as  $\tilde{t}_1$  is heavy ( $m_{\tilde{t}_1} \geq 120$  GeV), we may safely conclude that  $D_{g \rightarrow \tilde{H}}(z, Q^2) \sim 0$  when  $Q^2$  is not very great.

To precisely see the general behavior of the fragmentation function obtained, we draw its curves in Fig. 2. It can be found that when the mass of the top-squark becomes heavier, the peak of the curve for the fragmentation function increases to higher values accordingly.

Furthermore, to see the character of the fragmentation function obtained, let us compare it with those for the quarks ( $Q$ ). The fragmentation function for an antiquark  $\bar{Q}$  into a double heavy meson ( $\bar{Q}Q'$ ), e.g., a bottom-antiquark  $\bar{b}$  into  $B_c$ , which can be found in [22–28], is

$$D_{\bar{b}}(z) = F_{\bar{b}} \cdot f_{\bar{b}}(z), \quad (10)$$

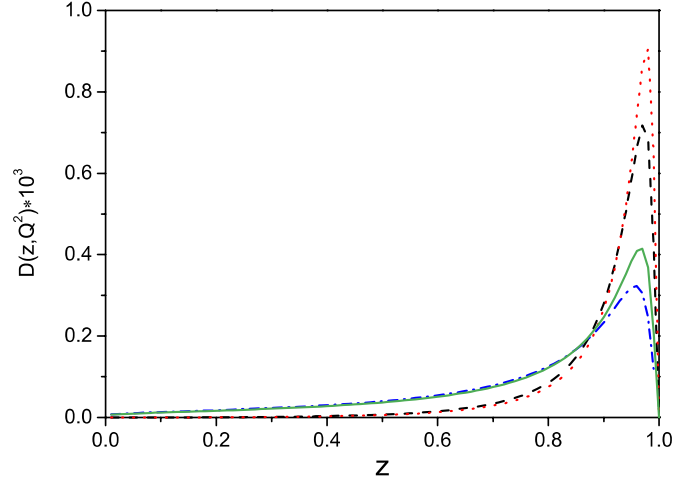


**Fig. 2.** Behavior of the fragmentation function (amplified by a scale factor  $10^3$  for convenience) for the light top-squark  $\tilde{t}_1$  to  $\tilde{H}$  (here  $\tilde{H}$  precisely indicates the  $S$ -wave  $(\tilde{t}_1 \bar{b})$  superhadron). The dotted and dashed lines stand for (5), the ‘initial’ fragmentation function, with  $m_{\tilde{t}_1} = 150$  GeV and  $m_{\tilde{t}_1} = 120$  GeV, respectively. The solid and dash-dot lines stand for the fragmentation function evolving to the energy scale  $Q = 2$  TeV (a typical energy scale) with  $m_{\tilde{t}_1} = 150$  GeV and  $m_{\tilde{t}_1} = 120$  GeV, respectively

where  $F_{\bar{b}} = \frac{8\alpha_s^2 |\psi_0(0)|^2}{27Mm_c^2}$  and

$$\begin{aligned} f_{\bar{b}}(z) &= \frac{z(1-z)^2}{(1-\lambda_1 z)^6} \\ &\times \left\{ [12\lambda_2 z - 3(\lambda_1 - \lambda_2)(1-\lambda_1 z)(2-z)](1-\lambda_1 z)z \right. \\ &\quad \left. + 6(1+\lambda_2 z)^2(1-\lambda_1 z)^2 - 8\lambda_1 \lambda_2 z^2(1-z) \right\}, \end{aligned} \quad (11)$$

where  $\psi_0(0)$  is the wavefunction at the origin of  $B_c$ ,  $\lambda_1 = \frac{m_b}{M}$ ,  $\lambda_2 = \frac{m_c}{M}$  and  $M = m_b + m_c$ . To highlight the difference between the two types of fragmentation functions, we remove the irrelevant factors  $F_{\bar{b}}$  and  $F_{\tilde{t}_1}$  and introduce the functions  $D'_b(z)$  and  $D'_s(z)$ :

$$D'_b(z) = f_{\bar{b}}(z) \text{ and } D'_s(z) = f_{\tilde{t}_1}(z).$$

One may see the differences clearly in the asymptotic behavior of the two kinds of fragmentation function, which for  $D'_b(z)$  and  $D'_s(z)$  are behaving as  $z$  and  $z^2$  as  $z \rightarrow 0$ , respectively; and the same,  $(1-z)^2$ , as  $z \rightarrow 1$ . Figure 3 depicts the two kinds of fragmentation function quantitatively. In the figure, the function  $D'_b(z)$  is taken precisely as the fragmentation function for the  $\bar{b}$ -quark fragmenting into a  $S$ -wave pseudoscalar state of the double heavy meson  $B_c$  or  $B_c^*$ , while the function  $D'_{\tilde{t}_1}(z)$  is the fragmentation function for the light top-squark  $\tilde{t}_1$  fragmenting into a  $S$ -wave superhadron  $\tilde{H} = (\tilde{t}_1 \bar{c})$ . In contrast with the difference between these two kinds of fragmentation function, in Fig. 3 we have artificially assumed  $m_{\tilde{t}_1} = m_b \simeq 5.18$  GeV.

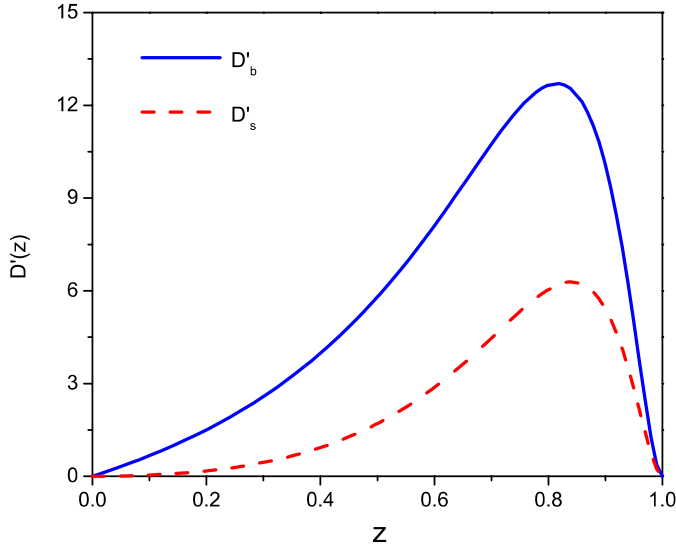


**Fig. 3.** Comparison of the two types of fragmentation functions. The *upper curve* (the *solid one*) is for  $D'_b(z)$ , and the *lower curve* (the *dashed one*) is for  $D'_s(z)$ . The relevant parameters are taken as  $m_{\tilde{t}_1} = m_b = 5.18$  GeV,  $m_c = 1.84$  GeV. The definitions and the artificial assumption are taken as in the text

### 3 Production of the superhadron at hadronic colliders

Here we are adopting the fragmentation approach to estimate the production of superhadrons at hadronic colliders. According to the NRQCD factorization theorem, the cross-section of  $\tilde{H}$  production by collisions of the hadrons  $H_1$  and  $H_2$ ,  $d\sigma_{H_1 H_2 \rightarrow \tilde{H} X}$ , can be factorized into three factors as follows:

$$d\sigma_{H_1 H_2 \rightarrow \tilde{H} X} = \sum_{ijk} \int dx_1 \int dx_2 \int dz f_{i/H_1}(x_1, \mu_f) f_{j/H_2}(x_2, \mu_f) \times d\hat{\sigma}_{ij \rightarrow kX}(x_1, x_2, z; \mu_f, \mu_R) \cdot D_{k \rightarrow \tilde{H}}(z, \mu_f), \quad (12)$$

where  $i, j$  and  $k$  are the parton species;  $\mu_f$  corresponds to the energy scale where the factorization is made;  $\mu_R$  is the renormalization energy scale for the hard subprocess;  $d\hat{\sigma}_{ij \rightarrow kX}(x_1, x_2, z; \mu_f, \mu_R)$  is the cross-section for the ‘hard subprocess’  $ij \rightarrow kX$ ;  $D_{k \rightarrow \tilde{H}}(z, \mu_f)$  is the fragmentation function of ‘parton’  $k$  to  $\tilde{H}$ ;  $f_{i/H_1}(x_1, \mu_f)$  and  $f_{j/H_2}(x_2, \mu_f)$  are the parton distribution functions (PDFs) in the colliding hadrons  $H_1$  and  $H_2$ , respectively. In this paper, as in most pQCD calculations, we choose  $\mu_f = \mu_R \sim \sqrt{m_{\tilde{H}}^2 + p_T^2}$ ,<sup>8</sup> and, as a consequence of this choice, we may further set  $D_{g \rightarrow \tilde{H}}(z, Q^2) = 0$  quite safely as argued above.

<sup>8</sup> One will see later on that the cross-section of the production rapidly decreases with  $p_T$ . Thus at Tevatron and LHC  $\mu_f = \mu_R \sim \sqrt{m_{\tilde{H}}^2 + p_T^2}$  is not high enough that  $m_{\tilde{t}_1}$  can be considered to be zero.

Therefore,  $k$  in (12) ‘runs over’  $\tilde{t}_1$  only, i.e.  $k = \tilde{t}_1$ . By naive considerations, of all the possible hard subprocesses for the production ( $ij \rightarrow kX, k = \tilde{t}_1$ ), gluon–gluon fusion  $g + g \rightarrow \tilde{t}_1 + \tilde{t}_1$  and quark–antiquark annihilation  $q + \bar{q} \rightarrow \tilde{t}_1 + \tilde{t}_1$  (here  $q$  and  $\bar{q}$  are light quarks) are of the same order in the strong coupling  $\alpha_s$ , so they may be the most important ones for production at the Tevatron and LHC colliders. The gluon component of the PDFs in the region of small  $x$  is greatest, so gluon–gluon fusion should be the most important one at LHC, whereas, at Tevatron, due to the comparatively low CM energy, the energy-momentum fraction  $x$  of the gluon parton must be large enough to produce a  $\tilde{t}_1 \tilde{t}_1$  pair, so as in the case of top-quark pair production at Tevatron, probably the components of the valence quarks, instead of the gluon, play a more important role (a review of this point can be found in [44]). Therefore, first of all we highlight these two subprocesses for the production. Note that according to [45] the production of the top-squark pair  $\tilde{t}_1 \tilde{t}_2$  or  $\tilde{t}_2 \tilde{t}_1$  at the hadronic colliders is small, so we do not take them into account. Now let us calculate the gluon–gluon fusion subprocesses first. To lowest order (tree level), there are four Feynman diagrams, as shown in Fig. 4. The corresponding amplitudes read

$$M_A = g_s^2 T^{ab} \frac{4p_1^\mu p_2^\nu \epsilon_\mu(k_1) \epsilon_\nu(k_2)}{(p_1 - k_1)^2 - m_{\tilde{t}_1}^2}, \quad (13)$$

$$M_B = g_s^2 T^{ba} \frac{4p_2^\mu p_1^\nu \epsilon_\mu(k_1) \epsilon_\nu(k_2)}{(p_1 - k_2)^2 - m_{\tilde{t}_1}^2}, \quad (14)$$

$$M_C = g_s^2 (T^{ab} - T^{ba}) \frac{(k_2 - k_1)^\mu g^{\mu\nu} - 2k_2^\mu g^{\mu'\nu} + 2k_1^\nu g^{\mu'\mu}}{(k_1 + k_2)^2} \times (p_1 - p_2)_{\mu'} \epsilon_\mu(k_1) \epsilon_\nu(k_2), \quad (15)$$

$$M_D = g_s^2 (T^{ab} + T^{ba}) \epsilon_\mu(k_1) \epsilon_\nu(k_2) g^{\mu\nu}. \quad (16)$$

where  $\epsilon$  is the polarization vector of the gluon. On taking the axial gauge with a fixed four-vector  $n$ , the summation of the polarization vector reads

$$\sum_\lambda \epsilon_\mu^*(k, \lambda) \epsilon_\nu(k, \lambda) = -g_{\mu\nu} - \frac{k_\mu k_\nu n^2}{(k \cdot n)^2} + \frac{k_\mu n_\nu + k_\nu n_\mu}{k \cdot n}.$$

The differential cross-section is

$$d\hat{\sigma}(gg \rightarrow \tilde{t}_1 \tilde{t}_1) = \frac{3\pi^2 \alpha_s^2}{16\pi \hat{s}^2} \left[ 1 - 2A - \frac{1}{9} \right] \times \left[ 1 - 2 \frac{m_{\tilde{t}_1}^2}{A \hat{s}} \left( 1 - \frac{m_{\tilde{t}_1}^2}{A \hat{s}} \right) \right] d\hat{t}, \quad (17)$$

where  $A = (\hat{t} - m_{\tilde{t}_1}^2)(\hat{u} - m_{\tilde{t}_1}^2)/\hat{s}^2$ .  $\hat{s}$ ,  $\hat{t}$  and  $\hat{u}$  are the Mandelstam variables of the subprocess,

$$\hat{s} = (k_1 + k_2)^2, \quad (18)$$

$$\hat{t} = (p_1 - k_1)^2, \quad (19)$$

$$\hat{u} = (p_1 - k_2)^2, \quad (20)$$

which satisfy  $\hat{s} + \hat{u} + \hat{t} = 2m_{\tilde{t}_1}^2$ . For the quark–antiquark annihilation subprocess, to the lowest order there is only one



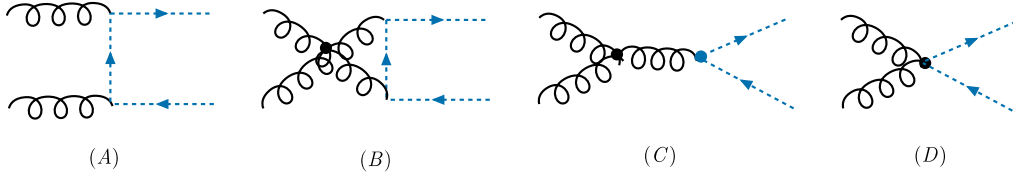


**Fig. 4.** The lowest order Feynman diagrams for the gluon–gluon fusion subprocess  $g + g \rightarrow \tilde{t}_1 + \tilde{t}_1^*$

**Table 2.** Hadronic cross sections (in units of fb) for the superhadrons  $(\tilde{t}_1 \bar{c})$  and  $(\tilde{t}_1 \bar{b})$  with  $J^P = (\frac{1}{2})^-$ . The parameters appearing in the estimate are taken as in the text

Constituents		LHC ( $\sqrt{S} = 14$ TeV)		TEVATRON ( $\sqrt{S} = 1.96$ TeV)	
		subprocess $gg$	subprocess $q\bar{q}$	subprocess $gg$	subprocess $q\bar{q}$
$m_{\tilde{t}_1} = 120$ GeV	$(\tilde{t}_1 \bar{c})$	114.51	0.36469	0.26975	1.2E-3
	$(\tilde{t}_1 \bar{b})$	30.489	0.10374	0.0696	3.E-4
$m_{\tilde{t}_1} = 150$ GeV	$(\tilde{t}_1 \bar{c})$	42.176	0.14591	0.0537	2.E-4
	$(\tilde{t}_1 \bar{b})$	11.812	0.0431	0.0142	7.E-5

Feynman diagram, and its Feynman amplitude reads

$$M_{q\bar{q} \rightarrow \tilde{t}_1 \tilde{t}_1^*} = g_s^2 T^{aa} \frac{(p_1^\mu - p_2^\mu) \bar{v}(k_2) \gamma_\mu u(k_1)}{(k_1 + k_2)^2}, \quad (21)$$

where  $k_1$  and  $k_2$  are the four-momenta for the quark and antiquark, respectively. The differential cross-section is obtained as follows:

$$d\hat{\sigma}(q\bar{q} \rightarrow \tilde{t}_1 \tilde{t}_1^*) = \frac{\pi \alpha_s^2 [\hat{s}^2 - 4\hat{s}m_{\tilde{t}_1}^2 - (\hat{t} - \hat{u})^2]}{9\hat{s}^4} d\hat{t}, \quad (22)$$

where the Mandelstam variables are defined in (18), (19) and (20). To calculate the production via the subprocess of quark–antiquark annihilation, as stated above, we are interested in considering the contributions of especially the

valence quarks, production at Tevatron, so here we are considering the contributions only from the light quarks in the PDFs to the production. In nucleons only the light quarks  $u$  and  $d$  may be their valence quarks.

The total hadronic cross-section is calculated via the two subprocesses in terms of the factorization formula (12) and with the help of the fragmentation function (5). The differential cross-section for gluon–gluon fusion is in terms of (17) and the differential cross-section for quark–antiquark annihilation is in terms of (22). Since the present calculations are at lowest order only, the CTEQ6L version [46] for the parton distribution functions (PDFs) has been taken, and, for definiteness, we take  $m_b = 5.18$  GeV and  $m_c = 1.84$  GeV and assume two possible values for  $m_{\tilde{t}_1}$ :  $m_{\tilde{t}_1} = 120$  or  $150$  GeV. In addition, the parameter  $\Lambda_{\text{QCD}}$  in the running coupling constant  $\alpha_s$  is taken as  $0.216$  GeV.

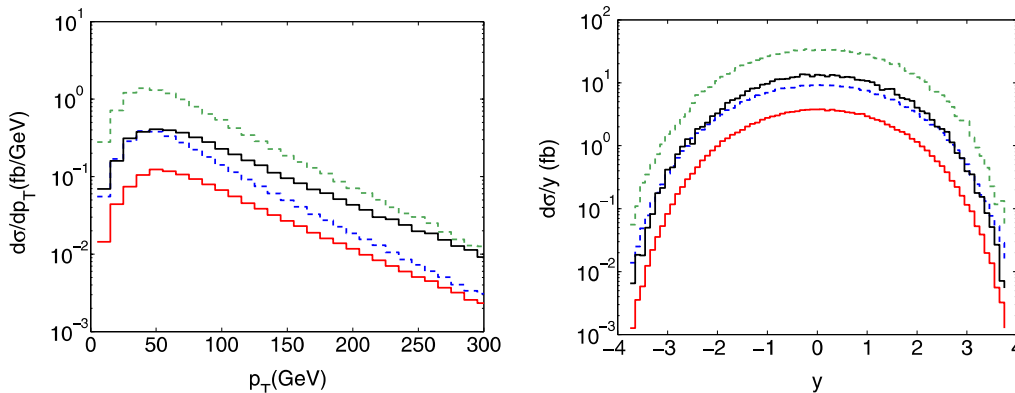


**Fig. 5.** The distributions of the transverse momentum  $P_T$  (left figure) and rapidity  $y$  (right figure) for the superhadron  $\tilde{H}$  produced via gluon–gluon fusion at LHC. For the  $P_T$  distribution, the rapidity cut  $|y| < 1.5$  is made. The *upper* one of the two *dash lines* corresponds to the distribution for superhadron  $(\tilde{t}_1 \bar{c})$  production with  $m_{\tilde{t}_1} = 120$  GeV being assumed, the *lower* one to that for superhadron  $(\tilde{t}_1 \bar{b})$  production with  $m_{\tilde{t}_1} = 120$  GeV; the *upper* one of the two *solid lines* to the distribution for superhadron  $(\tilde{t}_1 \bar{c})$  production with  $m_{\tilde{t}_1} = 150$  GeV, the *lower* one to the distribution for superhadron  $(\tilde{t}_1 \bar{b})$  production with  $m_{\tilde{t}_1} = 150$  GeV

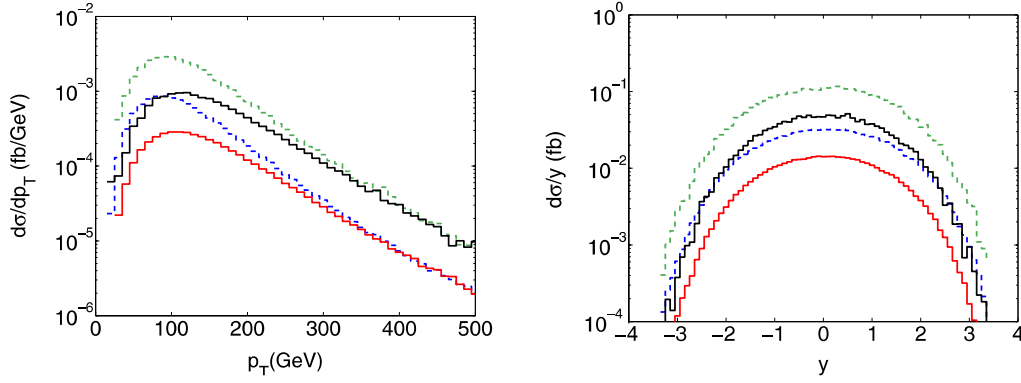


**Fig. 6.** The distributions of the transverse momentum  $P_T$  (left figure) and rapidity  $y$  (right figure) for the superhadron  $\tilde{H}$  produced via quark–antiquark annihilation at LHC. For the  $P_T$  distribution, the rapidity cut  $|y| < 1.5$  is made. The *upper* one of the two *dashed lines* corresponds to the distribution for superhadron  $(\tilde{t}_1\bar{c})$  production with  $m_{\tilde{t}_1} = 120$  GeV being assumed, the *lower* one to that for superhadron  $(\tilde{t}_1\bar{b})$  production with  $m_{\tilde{t}_1} = 120$  GeV; the *upper* one of the two *solid lines* to the distribution for superhadron  $(\tilde{t}_1\bar{c})$  production with  $m_{\tilde{t}_1} = 150$  GeV, the *lower* one to the distribution for superhadron  $(\tilde{t}_1\bar{b})$  production with  $m_{\tilde{t}_1} = 150$  GeV

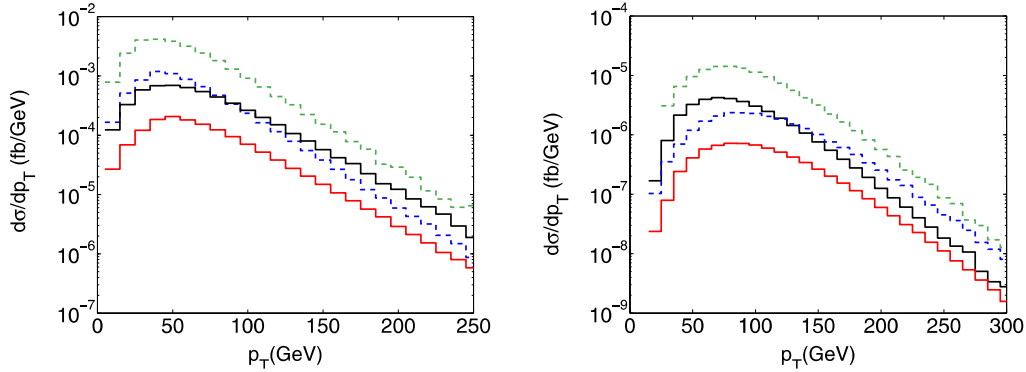


**Fig. 7.** The  $P_T$  distributions of the superhadrons  $\tilde{H}$  produced at Tevatron via gluon–gluon fusion (left figure) and quark–antiquark annihilation (right figure), respectively. For the distributions, the rapidity cut  $|y| < 0.6$  is made. The *upper* one of the two *dashed lines* corresponds to the distribution for superhadron  $(\tilde{t}_1\bar{c})$  production with  $m_{\tilde{t}_1} = 120$  GeV, the *lower* one to the distribution for superhadron  $(\tilde{t}_1\bar{b})$  production with  $m_{\tilde{t}_1} = 120$  GeV; the *upper* one of the *solid lines* to the distribution for superhadron  $(\tilde{t}_1\bar{c})$  production with  $m_{\tilde{t}_1} = 150$  GeV, the *lower* one to the distribution for superhadron  $(\tilde{t}_1\bar{b})$  production with  $m_{\tilde{t}_1} = 150$  GeV

The energy scale for the QCD factorization formulas is chosen as the ‘transverse mass’ of the produced superhadron:

$$\sqrt{m_{\tilde{H}}^2 + p_T^2}.$$

The total hadronic cross-sections obtained at Tevatron and LHC are in Table 2. From the table one may see that the cross-section for hadronic production of the superhadron  $\tilde{H}$  at Tevatron is much smaller than that at LHC (almost by three orders of magnitude), so when  $\tilde{t}_1$  shows the behavior as assumed here, and considering the final possible integrated luminosity, there is no hope to observe  $\tilde{H}$  at Tevatron, but it may be observed at LHC. Table 2 also shows that the hadronic cross-sections of the superhadron  $\tilde{H}$  at Tevatron and at LHC decrease as the mass of the light scalar top-quark  $m_{\tilde{t}_1}$  increases. Moreover, the cross-sections for superhadron production via gluon–gluon fusion are much larger than those via annihilation both at Tevatron and at LHC. Hence, the contribution from

quark–antiquark annihilation can be ignored in comparison to the dominant contribution from gluon–gluon fusion.

To present more features of the production, we also draw the curves showing the distributions of the produced superhadron. The differential cross-sections versus the transverse momentum  $p_T$  and the rapidity  $y$  of the produced superhadron via gluon–gluon fusion at LHC are drawn in Fig. 5, while those via quark–antiquark annihilation are drawn in Fig. 6. The distributions of the transverse momentum  $p_T$  for superhadron production at Tevatron via gluon–gluon fusion and quark–antiquark annihilation are drawn in Fig. 7 respectively.

## 4 Discussion and conclusions

Here the fragmentation function of the light top-squark  $\tilde{t}_1$  to heavy superhadrons  $(\tilde{t}_1\bar{c})$  and  $(\tilde{t}_1\bar{b})$  is as reliably com-



puted as in the case of a heavy quark to a double heavy meson. To see the characteristics of the fragmentation function, a comparison of the obtained fragmentation function for the light top-squark with those for heavy quarks is made by drawing the curves with suitable parameters in Fig. 3. When  $z$  approaches zero, the fragmentation functions for the top-squark (a scalar particle) approach zero as  $z^2$ , instead of those for a heavy quark (a fermion particle), which behave as  $z$ ; and both of them have a similar asymptotic behavior when  $z$  approaches 1.

Using the fragmentation function obtained for the superhadron  $\tilde{H}$  (either  $(\tilde{t}_1\bar{c})$  or  $(\tilde{t}_1\bar{b})$ ) and taking the fragmentation approach up to leading logarithm, the cross-sections and  $P_T(y)$  distributions for  $\tilde{H}$  have been computed at the energies of Tevatron and LHC. In the computation, gluon-gluon fusion and light quark-antiquark annihilation as the hard subprocess for the hadronic production of the superhadron  $\tilde{H}$  are taken into account in a precise way. When calculating the  $P_T$  distributions, different rapidity cuts are taken, i.e.  $|y| < 1.5$  at LHC and  $|y| < 0.6$  at Tevatron. From the cross-sections and  $P_T(y)$  distributions, one may conclude that one cannot collect enough events for observing the superhadron at the hadronic collider Tevatron, even if the parameters of the supersymmetric model are in a very favored region. On the contrary, enough events for the experimental observation of superhadrons can be produced (collected) without difficulty at the forthcoming LHC collider. Namely, if the expected ‘new physics’ is supersymmetric and the parameters are in the favored region of the superhadrons concerned and allowed by all kinds of existent experimental observations, Tevatron is not a good ‘laboratory’ to observe the possible superhadron(s), while LHC may be a good one. Moreover, it can be found from Table 2 that the production cross-section via  $q + \bar{q} \rightarrow \tilde{t}_1 + \tilde{t}_1$  is much smaller than that via the gluon-gluon fusion subprocess at Tevatron and LHC. To compare with the top-quark production, let us note here that quark-antiquark annihilation for top-quark production is comparable to gluon-gluon fusion at LHC [47–51]; for the top-quark, which is as heavy, the quark-antiquark annihilation mechanism is dominant over the gluon-gluon fusion at Tevatron [52–55]. So the cross-sections for single top production via  $q + \bar{q}' \rightarrow t + \bar{b}$  [56] and  $q + b \rightarrow q' + t$  [57], which are comparable to quark-antiquark annihilation, are also important for the top-quark production.

For the production of the superhadrons at Tevatron and at LHC, for the reason precisely pointed out in the above section, we have highlighted the two mechanisms via the hard subprocesses of gluon-gluon fusion and light quark-antiquark annihilation, so far. In fact, there may be some other mechanisms for producing the superhadrons, which may contribute more than via light quark-antiquark annihilation and may even be so sizable as to be comparable with that via gluon-gluon fusion. For instance, when a comparatively light chargino ( $m_{\tilde{\chi}^\pm} \leq \mathcal{O}(\text{TeV})$ ) is allowed in the same SUSY models, ‘single top-squark production’ such as that via  $g + b \rightarrow \tilde{t}_1 + \tilde{\chi}_{1/2}^-$  may occur: its contribution may be greater than that of light quark-antiquark

annihilation and may even be so sizable as to be comparable with that of gluon-gluon fusion. It is very similar to top production [47–51]: at the LHC single top production via the process  $g + b \rightarrow W + t$  has a cross-section of about 60 pb, while the cross-section via gluon-gluon fusion  $g + g \rightarrow t + \bar{t}$  is roughly about 760 pb, and the cross-section via quark-antiquark annihilation  $q + \bar{q} \rightarrow t + \bar{t}$  is roughly about 40 pb. Moreover, if the bottom-squark  $\tilde{b}_1$  is also comparatively light ( $m_{\tilde{b}_1} \leq \mathcal{O}(\text{TeV})$ ) in the same SUSY models, then production via  $q + \bar{q}' \rightarrow \tilde{t}_1 + \tilde{b}_1$  can be quite large too. However, all possibilities depend on the parameters of the relevant SUSY models; thus we could not calculate them precisely in this paper. As for the production via the subprocesses such as annihilation of the top-quark and antitop-quark through gluino  $\tilde{g}$  or photino  $\tilde{\gamma}$  exchanging,  $t + \bar{t} \rightarrow \tilde{t}_1 + \tilde{t}_1$ , and top-quark ‘scattering’ on a gluon,  $g + t \rightarrow \tilde{t}_1 + \tilde{g}(\tilde{\gamma})$  etc., we are sure that their contributions to superhadron production are very tiny due to the smallness of the PDF of the top-quark in the colliding hadrons. Anyway, for the accuracy of the present estimate and a ‘light’ top-squark with  $m_{\tilde{t}_1} = 120 \sim 150$  GeV, the contribution via the quark-antiquark annihilation hard subprocess to the production can be negligible in comparison to the dominant gluon-gluon fusion mechanism both at Tevatron and LHC, which is quite different from the top-quark case. Since the decay of the heavy superhadrons  $\tilde{H}$ , i.e.  $(\tilde{t}_1\bar{Q})$  with  $Q = c, b$ , is via the light top-squark  $\tilde{t}_1$  or via the involved heavy quark  $\bar{Q}$  with a proper relative decay possibility, there are two typical decay channels for  $\tilde{H}$ : one is the decay of the light top-squark  $\tilde{t}_1$  with the heavy quark  $\bar{Q}$  acting as a ‘spectator’, and the other is the decay of the heavy quark  $\bar{Q}$  with the light top-squark  $\tilde{t}_1$  acting as a ‘spectator’. The second decay channel may be quite different from that of the decay for a light top-squark  $\tilde{t}_1$  itself, and then it shall present certain characteristics. Therefore, we think that in order to observe and identify (discover) the light top-squark  $\tilde{t}_1$  experimentally, one may try to gain some advantage by observing the characteristics of the decay of the heavy  $\tilde{H}$  superhadrons.

If the heavy superhadrons are really observed experimentally, it will be good news not only for the relevant SUSY model(s) but also for the QCD-inspired potential model, because it will open a fresh field, i.e. the potential model will need to be extended to treat systems with binding of a fermion and a scalar boson.

As it is known, the fragmentation of a heavy quark  $b$  or  $c$  to a double heavy meson  $\eta_b$  or  $\eta_c$  is quite smaller than that of the heavy quark to a heavy  $B$  or  $D$  meson, i.e. with a relative possibility of about  $10^{-4} \sim 10^{-3}$  [22–28], and thus for the same reason one may be quite sure that the fragmentation function of the top-squark  $\tilde{t}_1$  to light superhadrons  $(\tilde{t}_1\bar{q})$ ,  $q = u, d, s$  is much greater than that of the top-squark  $\tilde{t}_1$  to heavy superhadrons  $(\tilde{t}_1\bar{Q})$   $Q = c, b$ . Namely, we conjecture that the fragmentation function of the top-squark  $\tilde{t}_1$  to light superhadrons  $(\tilde{t}_1\bar{q})$  may be about  $(10^3 \sim 10^4)$  of the one of the top-squark  $\tilde{t}_1$  to heavy superhadrons  $(\tilde{t}_1\bar{Q})$ . With an enhancement this large, the light superhadrons may be produced numerously, and then one

may collect enough events for experimental observation even at Tevatron. However, without the additional characteristics due to the decay to the heavy quarks  $b$  or  $c$  of the heavy superhadrons, the light superhadrons may be comparatively difficult to identify experimentally.

Finally, we should note here that the computation and discussion in the paper are explicitly based on the assumption that the light color-triplet top-squark does exist in certain SUSY models. As a matter of fact, the results in the present paper are true for a variety of SUSY models in which even the light top-squark  $\tilde{t}_1$  is not the lightest SUSY object with non-trivial color. As long as we are in the SUSY models concerned, the lightest SUSY partner is a scalar in a color triplet and has a lifetime long enough to form hadrons before decaying; our results as presented here remain meaningful by simply replacing the light top-squark  $\tilde{t}_1$  with the corresponding lightest SUSY partner.

*Acknowledgements.* This work was supported partly by the Natural Science Foundation of China (NSFC). The authors would like to thank J.M. Yang and J.P. Ma for helpful discussions.

## References

1. J. Wess, J. Bagger, *Supersymmetry and Supergravity* (Princeton University Press, Princeton, 1992)
2. S. Weinberg, *The Quantum Theory of Fields*, vol. 3 (Cambridge University Press, Cambridge, 1996)
3. H.P. Nills, *Phys. Rep.* **110**, 1 (1984)
4. H.E. Haber, G.L. Kane, *Phys. Rep.* **117**, 75 (1985)
5. Particle Data Group, S. Eidelman et al., *Phys. Lett. B* **592**, 1 (2004)
6. J. Ellis, K.A. Olive, Y. Santoso, V.C. Spanos, *Phys. Rev. D* **70**, 055005 (2004)
7. J.A. Aguilar-Saavedra et al., *Eur. Phys. J. C* **46**, 43 (2006) [and references therein]
8. J. Ellis, S. Rudaz, *Phys. Lett. B* **128**, 248 (1983)
9. M. Drees, K. Hikasa, *Phys. Lett. B* **252**, 127 (1990)
10. K.-I. Hikasa, M. Kobayashi, *Phys. Rev. D* **36**, 724 (1987)
11. W. Beenakker, R. Höpker, T. Plehn, P.M. Zerwas, *Z. Phys. C* **75**, 349 (1997)
12. C. Boehm, A. Djouadi, Y. Mambrini, *Phys. Rev. D* **61**, 095006 (2000)
13. A. Djouadi, Y. Mambrini, *Phys. Rev. D* **63**, 115005 (2001)
14. A. Djouadi, M. Guchait, Y. Mambrini, *Phys. Rev. D* **64**, 095014 (2001)
15. S.P. Das, A. Datta, M. Maity, *Phys. Lett. B* **596**, 293 (2004)
16. <http://lepsusy.web.cern.ch/lepsusy>
17. CDF Collaboration, T. Affolder et al., *Phys. Rev. Lett.* **88**, 041801 (2002)
18. D0 Collaboration, B. Abbott et al., *Phys. Rev. Lett.* **83**, 4937 (1999)
19. C.R. Nappi, *Phys. Rev. D* **25**, 84 (1982)
20. C.-H. Chang, J.Y. Cui, J.M. Yang, *Commun. Theor. Phys.* **39**, 197 (2003)
21. J.-K. Chen, Z.-Y. Fang, B.-Q. Hu, C.-H. Chang, *High Energy Phys. Nucl. Phys.* **26**, 766 (2002) (in Chinese)
22. C.-H. Chang, Y.-Q. Chen, *Phys. Lett. B* **284**, 127 (1992)
23. C.-H. Chang, Y.-Q. Chen, *Phys. Rev. D* **46**, 3845 (1992)
24. C.-H. Chang, Y.-Q. Chen, *Phys. Rev. D* **50**, 6013(E) (1994)
25. C.-H. Chang, Y.-Q. Chen, *Phys. Rev. D* **48**, 4086 (1993)
26. E. Braaten, K. Cheung, T.C. Yuan, *Phys. Rev. D* **48**, 4230 (1993)
27. E. Braaten, K. Cheung, T.C. Yuan, *Phys. Rev. D* **48**, R5049 (1993)
28. V.V. Kiselev, A.K. Likhoded, M.V. Shevlyagin, *Z. Phys. C* **63**, 77 (1994)
29. G.T. Bodwin, E. Braaten, G.P. Lepage, *Phys. Rev. D* **51**, 1125 (1995)
30. G.T. Bodwin, E. Braaten, G.P. Lepage, *Phys. Rev. D* **55**, 5853 (1997) [Erratum]
31. L. Clavelli, *Phys. Rev. D* **26**, 1610 (1982)
32. C.-R. Ji, F. Amiri, *Phys. Rev. D* **35**, 3318 (1987)
33. C.-H. Chang, Y.-Q. Chen, G.-P. Han, H.-T. Jiang, *Phys. Lett. B* **364**, 78 (1995)
34. C.-H. Chang, Y.-Q. Chen, R.J. Oakes, *Phys. Rev. D* **54**, 4344 (1996)
35. K. Kolodziej, A. Leike, R. Rückl, *Phys. Lett. B* **355**, 337 (1995)
36. G. Altarelli, G. Parisi, *Nucl. Phys. B* **126**, 298 (1977)
37. V.N. Gribov, L.N. Lipatov, *Yad. Fiz.* **15**, 781 (1972)
38. Y.L. Dokshitzer, *Sov. Phys. JETP* **46**, 641 (1977)
39. C. Kounnas, D.A. Ross, *Nucl. Phys. B* **214**, 317 (1983)
40. S.K. Jones, C.H. Llewellyn Smith, *Nucl. Phys. B* **217**, 145 (1983)
41. S. Kraml, hep-ph/9903257
42. E.J. Eichten, C. Quigg, *Phys. Rev. D* **52**, 1726 (1995)
43. R.D. Field, *Applications of Perturbative QCD* (Addison-Wesley, New York, 1989)
44. W. Wagner, *Rep. Prog. Phys.* **68**, 2409 (2005)
45. W. Beenakker, M. Kramer, T. Plehn, M. Spira, P.M. Zerwas, *Nucl. Phys. B* **515**, 3 (1998)
46. J. Pumplin, D.R. Stump, J. Huston, H.L. Lai, P. Nadolsky, W.K. Tung, *JHEP* **0207**, 12 (2002)
47. E.L. Berger, H. Contopanagos, *Phys. Rev. D* **57**, 253 (1998)
48. R. Bonciani, S. Catani, M.L. Mangano, P. Nason, *Nucl. Phys. B* **529**, 424 (1998)
49. N. Kidonakis, R. Vogt, *Phys. Rev. D* **65**, 014012 (2002)
50. E.L. Berger, H. Contopanagos, *Phys. Rev. D* **54**, 3085 (1996)
51. S. Frixione, M.L. Mangano, P. Nason, G. Ridolfi, hep-ph/9702287
52. M. Cacciari, S. Frixione, M.L. Mangano, P. Nason, G. Ridolfi, *JHEP* **0404**, 68 (2004)
53. N. Kidonakis, R. Vogt, *Phys. Rev. D* **68**, 114014 (2003)
54. S. Catani, M.L. Mangano, P. Nason, L. Trentadue, *Phys. Lett. B* **378**, 329 (1996)
55. S. Catani, M.L. Mangano, P. Nason, L. Trentadue, *Nucl. Phys. B* **478**, 273 (1996)
56. S. Cortese, R. Petronzio, *Phys. Lett. B* **253**, 494 (1991)
57. S. Willenbrock, D. Dicus, *Phys. Rev. D* **34**, 155 (1986)